

Chapter 3 . Fundamental mechanics of hair cell bundles

Bundles differ between species, organs, and even locations within the same organ. Variations include cilia diameter, height, rate of height drop-off, and number of cilia. Because of their small size, interconnections have been even more elusive to characterize. Their number, distribution, diameter, length and material type have yet to be determined. Some general principles of hair cell bundle mechanics allowing us to compare structural variations is needed. This chapter hopes to discover these mechanical principles.

In an effort to understand the fundamental mechanics of hair cell bundles, I have analyzed simple cilia and interconnection structures, studying the effects of changes in stereocilium stiffness, height distribution, and the configuration and composition of the interconnections.

Furthermore, there may be some factors that are not very important to predicting bundle response. It is hoped that we may find which variations in bundles effect large changes in stiffness and link tension from a mechanical standpoint, which are more robust, and which are irrelevant. This can direct biological investigation towards quantifying the most important mechanical features of hair cell bundles.

Bundle stiffness (resistance to deflection) and link tension will be the primary mechanical aspects that will be studied. Also investigated will be the change in deformation shape.

I start with a single stereocilium under a transverse point load. This will give a reference point for later calculations. The study then expands to two cilia, and then several cilia in a column. Cases will be investigated with one link between neighboring cilia, then two, and then many. I will also investigate the case of two cilia linked together and forced off-axis.

Single stereocilia

The simplest model is a single forced cilia, removed from the rest of the bundle. This model approximates the cilia as a cantilever beam of constant cross section (figure 3-1).

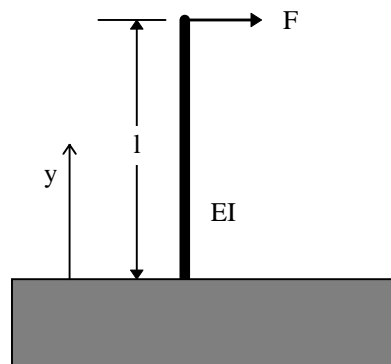


Figure 3-1. Single stereocilium (cantilevered beam) under a point load.

The solution for transverse deflection of a cantilever beam under a point load is

$$w(y) = \frac{F}{EI} \frac{y^2}{2} \left(l - \frac{y}{3} \right) \quad (3.1)$$

where E is Young's modulus and I is the moment of inertia of the cross section, which because we have a circular cross section, is

$$I = \frac{\pi}{64} d^4$$

where d is the ciliary diameter. The deflection at the tip (defined as y=l) is

$$w(l) = \frac{Fl^3}{3EI} \quad (3.2)$$

and the stiffness, k_s , defined as the quotient of the applied force and the tip deflection is

$$k_s = \frac{F}{w(l)} = \frac{3EI}{l^3}. \quad (3.3)$$

From equation 3.3 it can be seen ciliary stiffness increases with increasing diameter and decreases with increasing height. This single stereocilium stiffness will be essential as both link stiffness and bundle (or ciliary-link assembly) stiffness will be nondimensionalized by this value.

The next step in adding complexity to our model is to include shear deformability. As discussed earlier, stereocilia have been observed to undergo large amounts of shear deformation. An independent shear modulus, G, is introduced to the constant diameter stereocilia studied above. The stiffness of a shear deformable stereocilia compared to the isotropic cilia is

$$\frac{k_s}{k_{s-isotropic}} = \left[1 + \frac{3}{16} \frac{\bar{d}^2}{\bar{G}} \right]^{-1} \quad (3.4)$$

where

$$\bar{G} = \frac{GK}{E} \quad (3.5)$$

$$\bar{d} = \frac{d}{l}$$

with K denoting the shear correction factor and d indicating the diameter of the cilia.

The shear modulus has a maximum value when the ciliary material is isotropic. This value is one-half to one-third of the material's Young's modulus, depending upon Poisson's ratio. The ciliary stiffness as a function of shear modulus (normalized by the isotropic stereocilium of equation 3.3) is plotted as curve A in figure 3-2. The chosen ciliary diameter for this plot reflects a biologically realistic scenario of a cilium 10 μm tall and 0.2 μm in diameter.

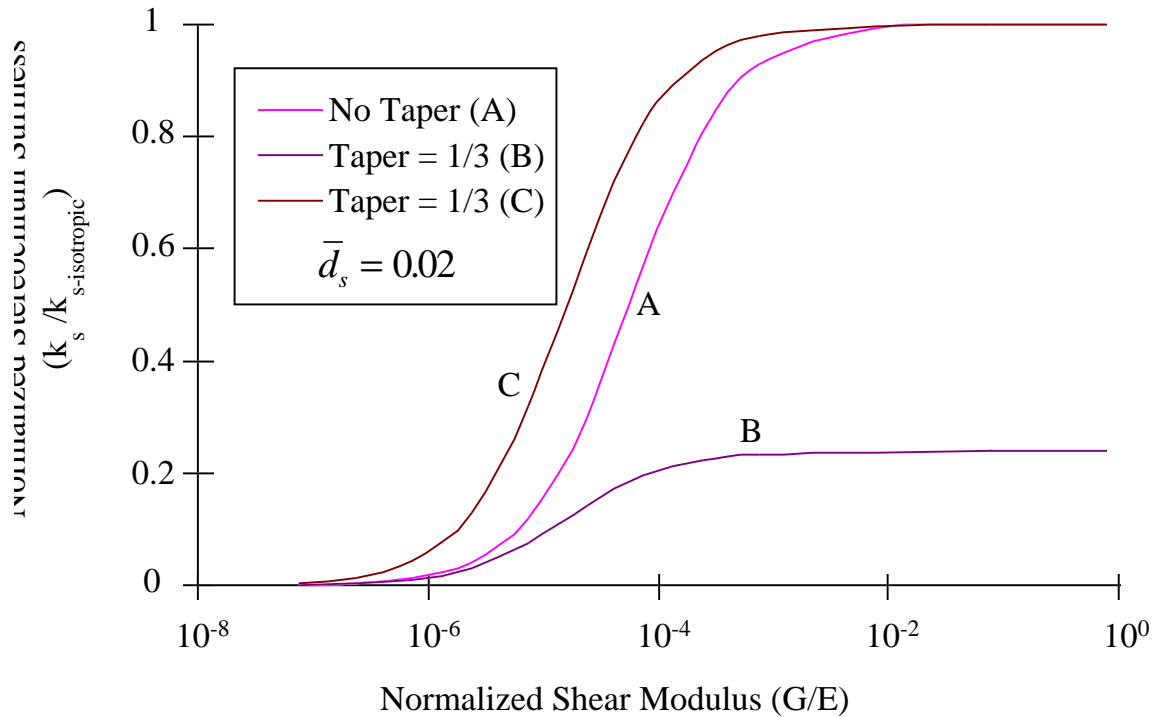


Figure 3-2. Plot of ciliary stiffness versus shear modulus for an A) untapered base and B) tapered base stereocilia. Curve C) depicts the same tapered base stereocilia in curve B) only it is normalized by a tapered base isotropic stereocilia. This indicates the taper both decreases stiffness, and shifts the stiffness/shear modulus curve to the left.

As the shear modulus is reduced, it originally has little to no effect. Between G/E of 10^{-2} to 10^{-3} the effect is minor, but noticeable. From 10^{-3} to 10^{-5} stiffness drops rapidly. Below 10^{-5} the shear dominates.

Another effect of reduced shear modulus is seen when the deformed profile of the stereocilia is examined (Figure 3-3). By increasing shear deformation, the stereocilia exhibits a less curved deflection profile for the same tip deflection.

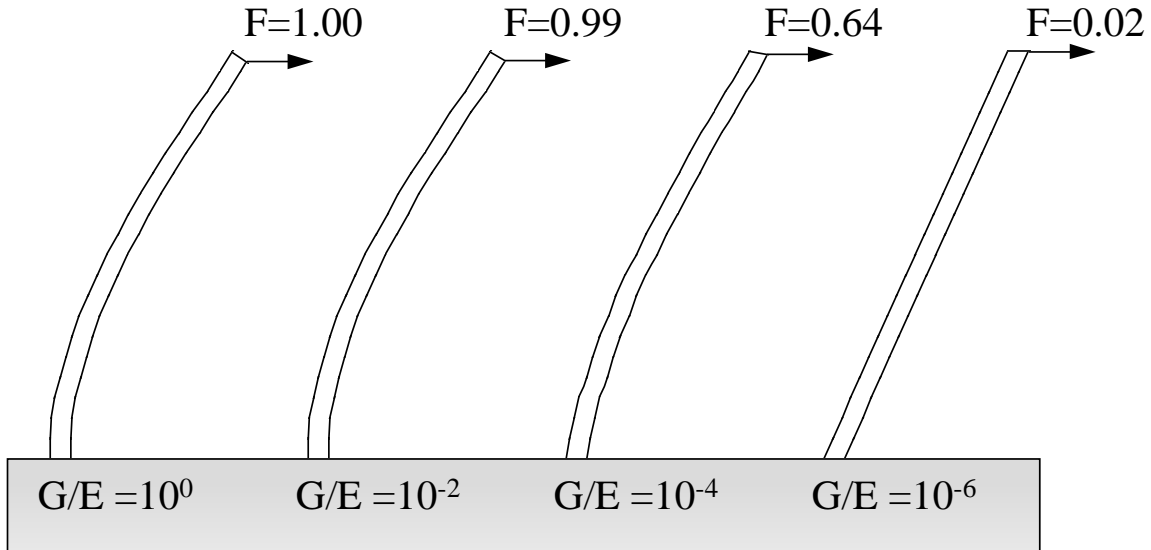


Figure 3-3. Deflection profiles for different values of G/E for nontapered base cilia ($d/l = 0.02$). The force depicted at the top indicates the relative force needed to produce identical tip deflections.

The last modification I will make to the single stereocilia model is to taper its base. As discussed in chapter 1, all stereocilia exhibit a decrease in diameter as they near their base. Using the bundle modeler program, *bmod*, a single stereocilia was modeled with a tapered base. To imitate biologic reality, the cilia tapers at the last ten percent of its height to an insertion point where its diameter is one-third of its original diameter.

Curve B in figure 3-2 depicts the relationship between stiffness and shear modulus for this stereocilia. Curve B shows that for values of G/E greater than 10^{-3} , the cilium loses 23 percent of its stiffness when compared to an untapered cilium. By normalizing the stiffness of our anisotropic tapered cilium with that of an isotropic tapered cilium, as depicted in curve C, we see a secondary effect. The tapered base increases the bending deformation at the base, diminishing the effect of a reduced shear modulus by nearly a decade when compared to an untapered cilium.

The effect of a tapered base on the deformation profile is shown in Figure 3-4. By tapering the base, more deformation due to bending occurs at the base, making the rest of the shaft relatively stiffer. The result is a flatter profile, as described in biological deformations as stereocilia pivoting about their base (Tilney, 1983).

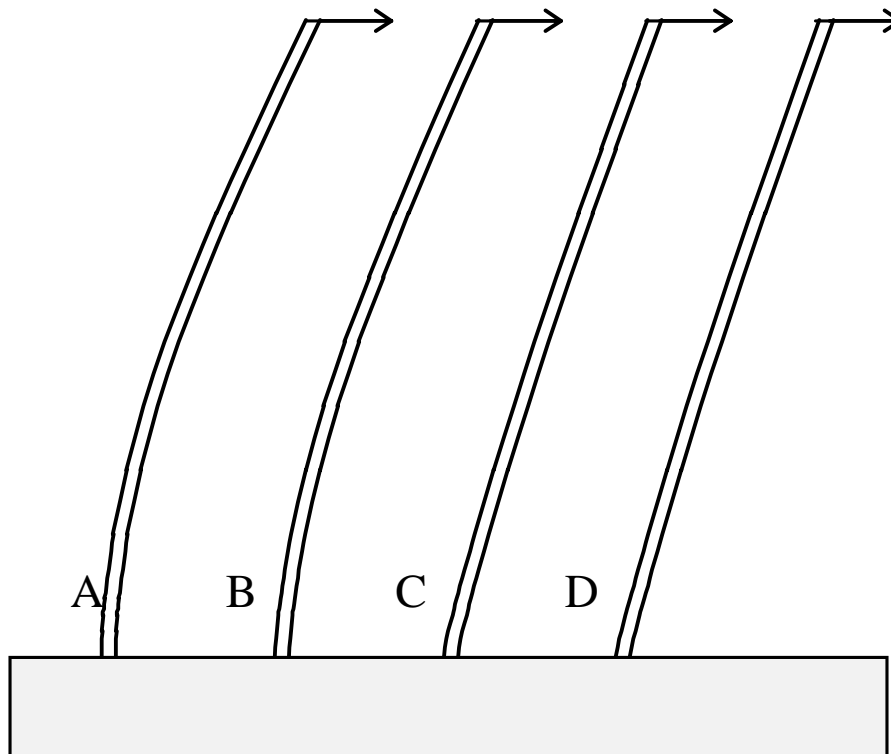


Figure 3-4 Deflection profiles of four stereocilia with identical tip deflections ($d/l = 0.02$). A has an untapered base and is isotropic, B is untapered and anisotropic, C is tapered and isotropic, D is tapered and anisotropic. Anisotropic stereocilia have $G/E = 10^{-3}$. Tapered stereocilia have linearly reducing diameters in the bottom 10 percent of length to one third of the original diameter.

The overall effect of combining shear deformability with a tapered base is a reduction in cilia stiffness (which corresponds to a loss in bundle stiffness) and a more linear deflection profile.

Two stereocilia connected by one link

The next step up in complexity is to add a second cilia and connect the two by a single link, as seen in Figure 3-5. We start with the most simple components— isotropic, untapered stereocilia. The stereocilia have heights l_1 and l_2 , while the single link has a stiffness of k_1 . The force is applied to the top of the tallest stereocilia.

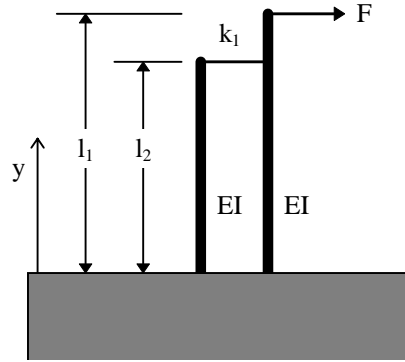


Figure 3-5. Two stereocilia connected by a single link.

The tension in the link, normalized by the applied force is found to be

$$\bar{g} = \frac{g}{F} = \frac{\Omega}{\bar{k}_l^{-1} + 2\bar{l}_2^3} \quad (3.6)$$

where,

$$\bar{k}_l = \frac{k_l}{k_s} = \frac{k_l l_1^3}{3EI} \quad (3.7)$$

and Ω is a geometric parameter that can be interpreted as the ratio of deflection at the height of the link (l_2) divided by the deflection at the tip (l_1) for a system with no link stiffness, or

$$\Omega = \frac{w(l_2)}{w(l_1)} \Big|_{k_l=0} = \frac{\bar{l}_2^2}{2} (3 - \bar{l}_2) \quad (3.8)$$

The nondimensional stiffness of the assembly is

$$\bar{k}_b = \frac{\bar{F}}{\bar{w}(1)} = \left[1 - \frac{\Omega^2}{\bar{k}_l^{-1} + 2\bar{l}_2^3} \right]^{-1} \quad (3.9)$$

Plots of the link tension and assembly stiffness as a function of link stiffness are presented in figures 3-5 and 3-6, respectively.

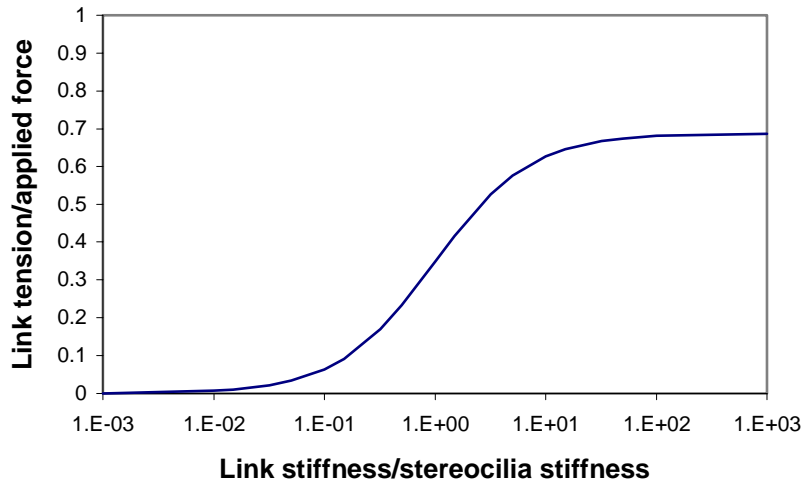


Figure 3-6. Link Tension as a function of link stiffness for the two stereocilia/one link scenario. ($I_2/I_1 = 0.8$)

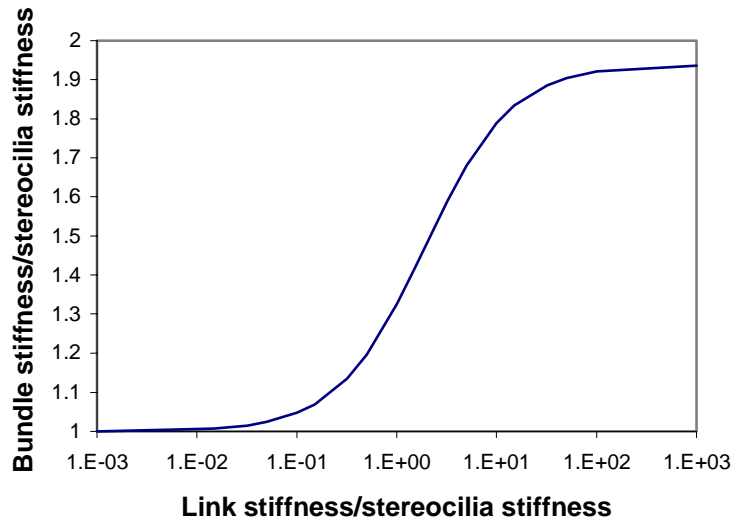


Figure 3-7. Assembly stiffness as a function of link stiffness for the two stereocilia-one link scenario. ($I_2/I_1 = 0.8$)

Even this simple case gives us a tremendous amount of insight into the problem. For a compliant link (figure 3-8 A), the bundle stiffness equals that of a single stereocilium. The link stretches easily, absorbing very little energy because of its small stiffness. It also passes along a negligible force to the second stereocilium. The energy of the applied force is absorbed solely by deformation of the first stereocilium.

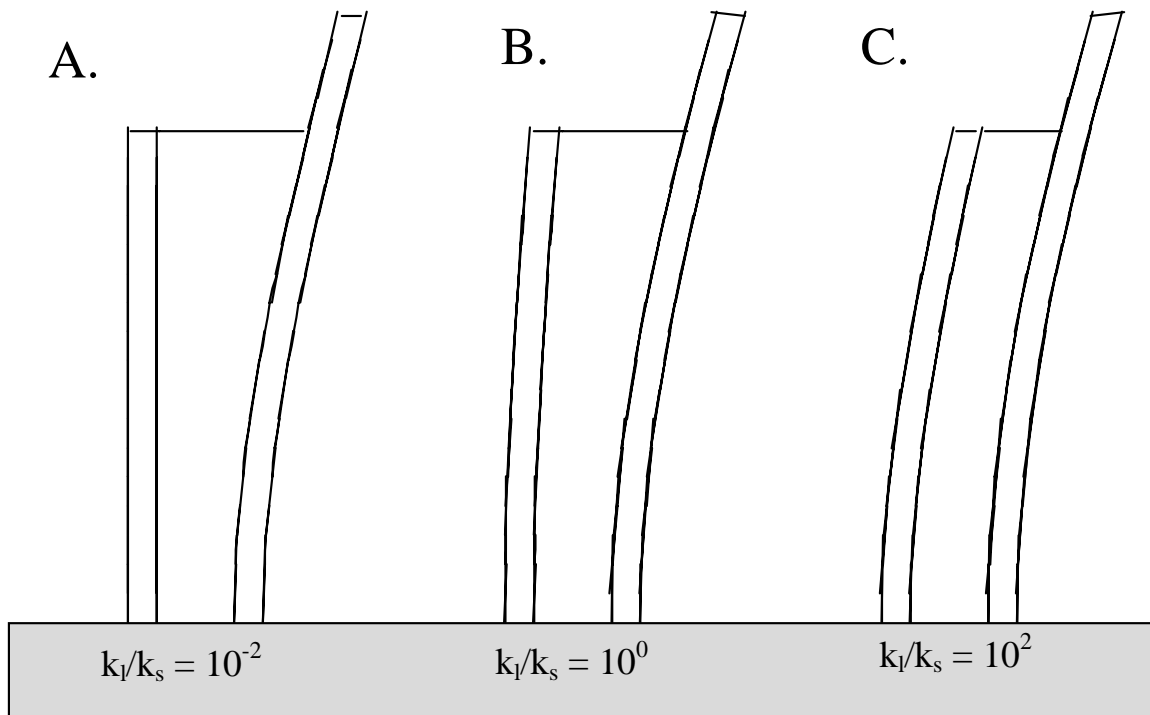


Figure 3-8 Deformation profiles for three values of nondimensional link stiffness. ($l_2/l_1 = 0.8$)

As the link gets stiffer, the link tension does increase. Some force is being shared with the second stereocilium. However, the still compliant link stretches, causing a larger deflection of the first stereocilium (figure 3-8 B).

Finally, once a certain link stiffness is attained, when a force is applied to the tall cilia, the tension saturates. The bundle deforms as a single unit (figure 3-8 C). This mode of deformation is the only one observed biologically. While the minimum link stiffness value for this model ($k_l = 100 k_s$) may not be indicative of that for an actual bundle (with an array of anisotropic tapered stereocilia and multiple links), it does alert us to the fact that a minimum stiffness value for links does exist and should be identified. This allows us to discount certain geometric and material properties as being present in links.

A last investigation of the second simple model will focus on the height of the second stereocilium. Figure 3-9 below shows the effect of the height of the second stereocilia on both the assembly stiffness and the link tension for an infinitely stiff link (i.e. equation 3-6 and 3-9 for $k_l/k_s \rightarrow \infty$). It can be seen as the second stereocilium grows in height, its contribution to assembly stiffness grows. On the other hand, the tension in the link is inversely proportional to height. Noticeable is the increase in tension several times that of the applied force in sharper drop-offs. Therefore, bundles with great drop-offs in stereocilia height magnify the applied force and may be more sensitive transducers.

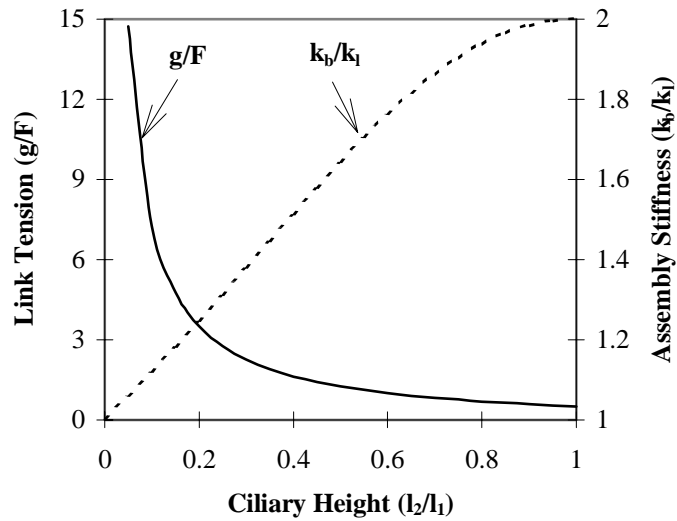


Figure 3-9. Effect of the second ciliary height on link tension and assembly stiffness. ($k_i/k_s \rightarrow \infty$)

Once again, we do the same tests as above using the *bmod* program to make the component stereocilia more realistic. When bundle stiffness is plotted as a function of link stiffness (figure 3-10 below) the curve follows the same relationship as the isotropic, constant cross section case. The magnitude of stiffness increase given by the second stereocilia decreases somewhat, but the results do indicate that the link stiffness must be an order of magnitude greater than stereocilia stiffness.

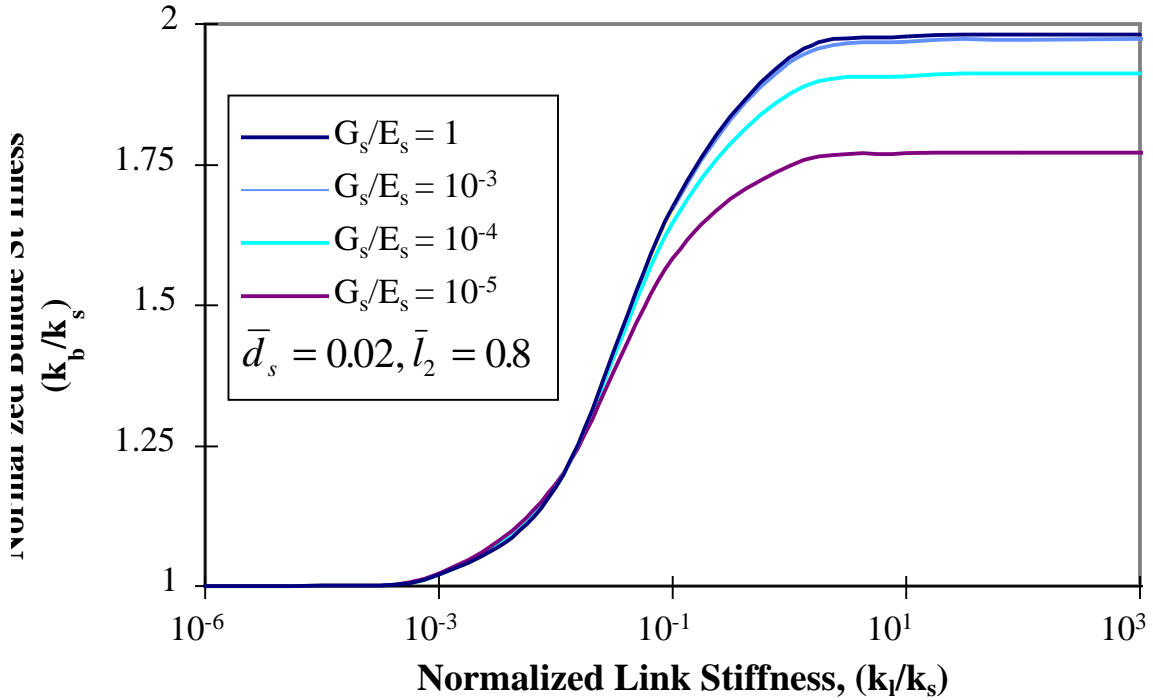


Figure 3-10. For two biologically realistic stereocilia connected by a single link, the effect of lowering the shear modulus on the relationship between link stiffness and bundle stiffness.

A column of cilia each connected by a single link

The next scenario features many stereocilia, each connected by a single link, as depicted in the figure 3-11 below.

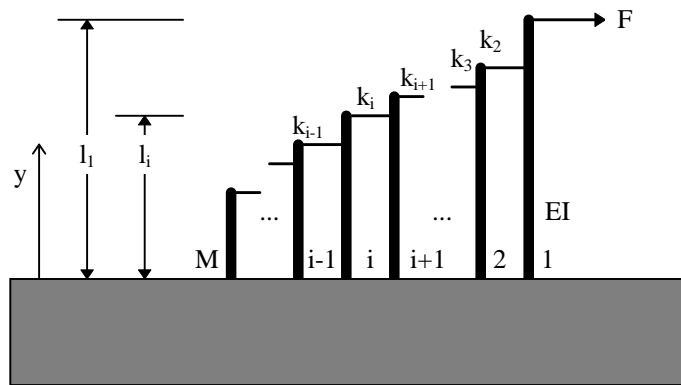


Figure 3-11 Column of singly linked stereocilia.

For the following results, link stiffnesses, ciliary moduli, and ciliary radii were assumed constant across the column. Using a linear drop-off in stereocilia height, where each successive stereocilium is reduced in height by $1/10^{\text{th}}$ the height of the tallest stereocilium (i.e. relative

heights of 10, 9, 8, 7, etc.), the following results were generated and are presented in the figures below.

Figure 3-12 depicts the assemblage stiffness as a function of column length. Different curves represent different values of link stiffness, k_l . Figure 3-13 depicts the same data only the assembly stiffness is plotted with link stiffness on the ordinate axis. Different column lengths are shown as different curves.

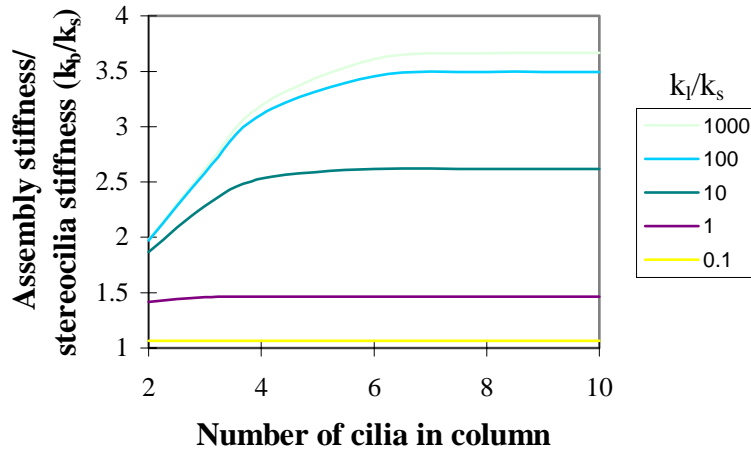


Figure 3-12. For a column of singly linked stereocilia, stiffness plotted against column length for different link stiffnesses.

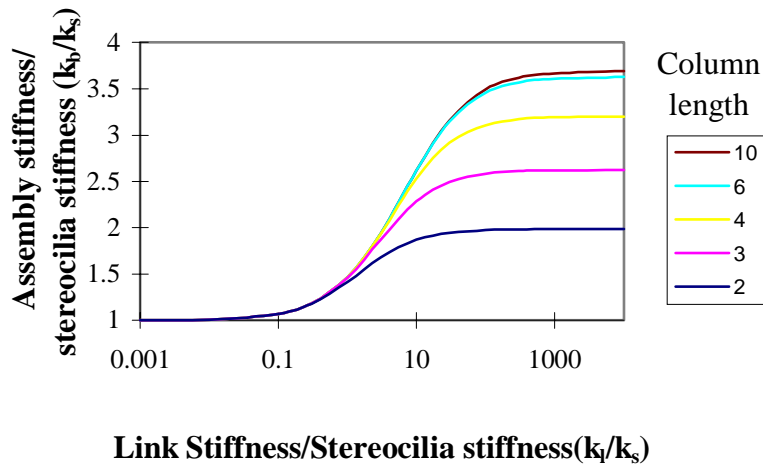


Figure 3-13. Bundle stiffness versus link stiffness for various lengths of columns.

The most noticeable thing in this scenario is the effect of lengthening the column. As seen earlier, the stiffness of a stiffly linked two cilia model approaches the stiffness of two cilia. As the third and fourth cilia are added, stiffness increases almost linearly. Then as more cilia are

added to the column, the effect decreases. Beyond the sixth or seventh cilia, adding more cilia has no effect on bundle stiffness, regardless of link stiffness.

These results confirm models done for more biologically realistic bundle columns [Peterson et. al., 96]. In those studies, the cilia were tapered, anisotropic, and followed height distributions that describe actual bundle types.

Further interest may be found in the tensions of each link. In figure 3-14 we show the tension in links of long columns. Note how link tension drastically drops off.

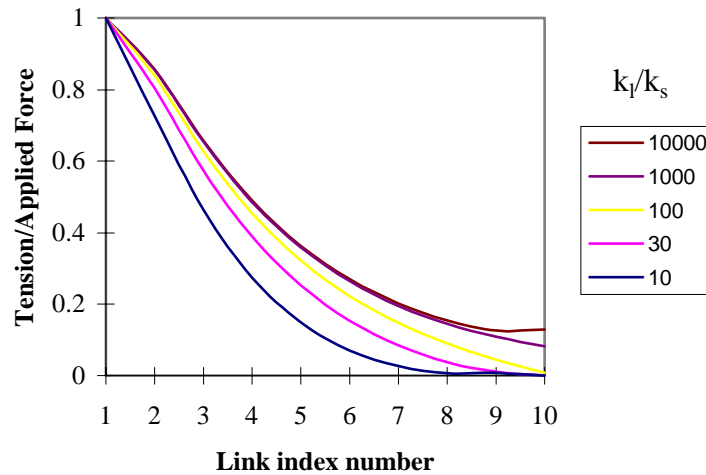


Figure 3-14. Link tension versus link number for different link stiffness values. Tension 1 reflects the applied force, hence is unity.

Two stereocilia connected by two links

We next study the case of two beams linked by two links (Figure 3-15). This is relevant as stereocilia are connected by a number of links extending down their length.

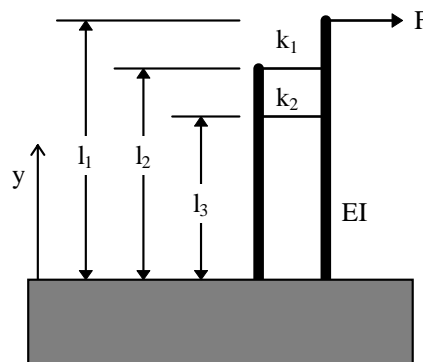


Figure 3-15 Two beams connected by two links

As presented in the previous chapter, the link tensions are

$$\bar{g}_1 = \frac{\Omega_{12}(k_2^{-1} + 2l_2^3) - 2\Omega_{13}\Omega_{23}l_2^3}{(k_1^{-1} + 2l_2^3)(k_2^{-1} + 2l_2^3) - (2l_2^3\Omega_{23})^2} \quad (2.11)$$

$$\bar{g}_2 = \frac{\Omega_{13}(k_1^{-1} + 2l_2^3) - 2\Omega_{12}\Omega_{23}l_2^3}{(k_1^{-1} + 2l_2^3)(k_2^{-1} + 2l_2^3) - (2l_2^3\Omega_{23})^2}$$

where

$$\Omega_{ij} = \frac{1}{2} \left(\frac{l_j}{l_i} \right)^3 \left(3 \frac{l_i}{l_j} - 1 \right) \quad (2.10)$$

and the stiffness of this assembly is

$$\bar{k}_b = \left\{ 1 - \frac{\Omega_{12}^2(\bar{k}_2^{-1} + 2\bar{l}_3^3) + \Omega_{13}^2(\bar{k}_1^{-1} + 2\bar{l}_2^3) - 4\bar{l}_2^3\Omega_{12}\Omega_{13}\Omega_{23}}{(\bar{k}_1^{-1} + 2\bar{l}_2^3)(\bar{k}_2^{-1} + 2\bar{l}_3^3) - (2\bar{l}_2^3\Omega_{23})^2} \right\}^{-1} \quad (2.12)$$

It can be seen that as the second link stiffness vanishes (k_2 approaches 0) the stiffness matches that of the single link system presented earlier.

By plotting the relative tension of the second link for different link heights (figure 3-16), it can be seen that as the second link is placed lower, its tension decreases. As the links stiffen, the second link tension gets smaller. For a link stiffness ten times that of the stereocilia, it can be seen that a second link must be near the first at the top of the cilia to carry any load, and therefore be mechanically relevant.

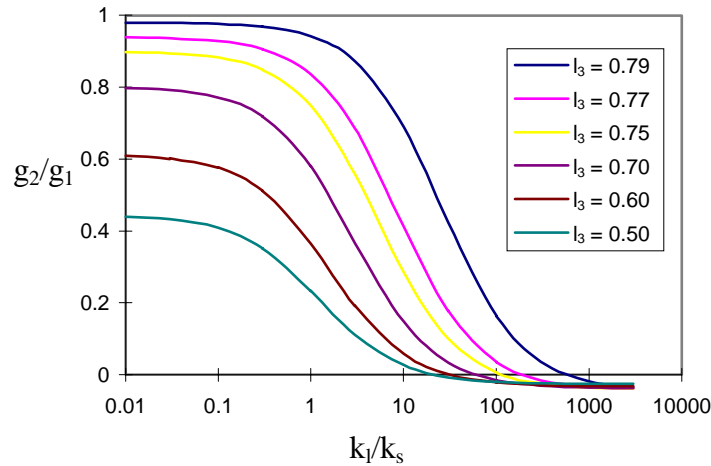


Figure 3-16. Relative link tensions in the two stereocilia, two-link scenario. (Corresponding heights for l_3 are $l_1=1.0$, $l_2 = 0.8$. Link stiffness is constant $k_1 = k_1=k_2$.)

While this model lacks several biologically realistic features (notably tapered base, anisotropy) that would flatten the deflection profile and lessen this effect, the general principle is

that successive lateral links will lose mechanical relevance if the links are (1) relatively stiff and (2) placed low on the ciliary shaft.

To verify the above conclusions for more biologically realistic stereocilia, *bmod* was used to simulate the above two cilia with heights of 10 and 8 μm and diameters of 0.2 μm . The ciliary base tapers to one third of the body diameter in last 1 μm of ciliary height and the shear modulus is equal to 10^{-3} Young's modulus.

The results are depicted in figure 3-17. Although in general, compared to the closed form solution with the simplified stereocilia, this model maintains tension in the second link longer, it is clear that even for the flatter deformation profiles of realistic cilia, there is a reduction in mechanical effectiveness when links are placed lower on the cilia.

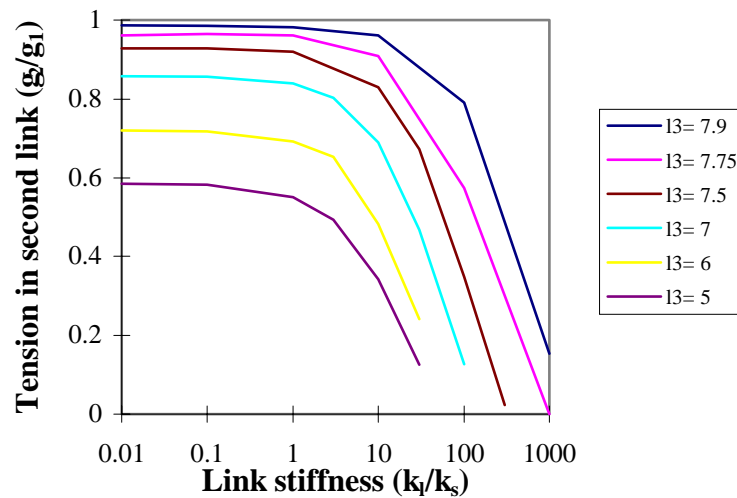


Figure 3-17. Link tension results of two cilia, two-link model on biologically realistic cilia.

Two cilia connected by many links

The next scenario studied is the solution of two stereocilia connected by several links (Figure 3-17). There are N links, each attached at a height, h_i , each with a link stiffness of k_i .

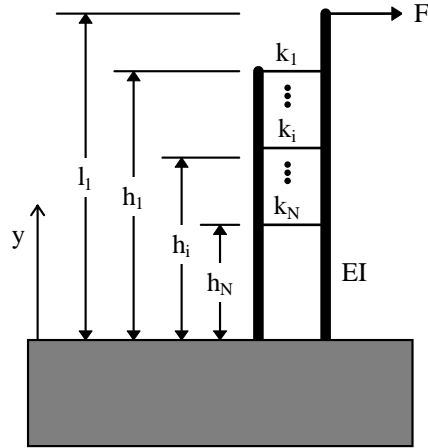


Figure 3-18. Multiply linked two stereocilia bundle.

Bundle stiffness was determined for assemblies with one to ten links of constant stiffness, $k_1 = k_2 = \dots = k_N = k_l$. The second stereocilium height was 80 percent of the first. Links were placed, starting at the top of the second stereocilium with each additional one slightly lower (2.5 percent of the tallest stereocilia height, l_1). Because we assume the links are thin strands of proteins, incapable of supporting a compressive load, any case resulting with a link in compression was redone with that link removed. The effect of link stiffness was also investigated in these assemblies.

Figure 3-19 plots the now familiar link stiffness versus assembly stiffness curve, only with a variable number of links. The difference is most pronounced when the link stiffness is in the intermediate range (0.1 to 10 times the stereocilium stiffness). Even then, there is little effect on assembly stiffness when adding more than four or five links. For stiff links, successive links have little effect.

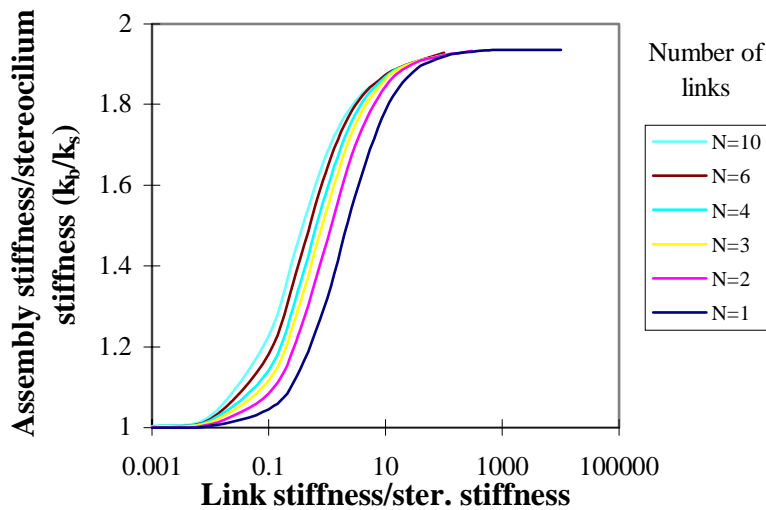


Figure 3-19. Assembly stiffness versus link stiffness for multiply linked two stereocilia scenario.

Figure 3-20 depicts the same data, only with different curves representing relative link stiffness and the ordinate axis depicting the number of links. Noticeable here is the diminishing mechanical effect of adding links. Even for slightly stiff links ($k_l/k_s = 10$) adding more than 3 links has no effect.

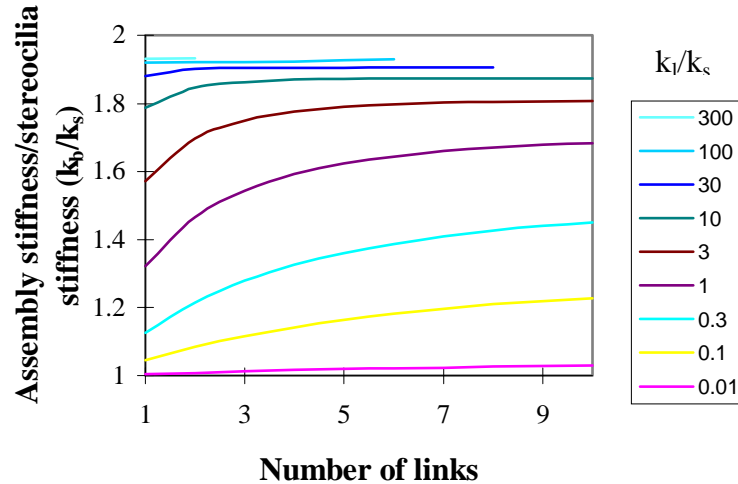


Figure 3-20. Assembly stiffness versus number of links for multiply linked two stereocilia scenario. The top three cases ($k_l/k_s = 300, 100, 30$) do not extend to the full 10 links because the lower links become in a state of compression. Such cases are considered an artifact of the model as biological links are thin strands of protein, unable to carry compressive forces.

Examining the tension in these links (figure 3-21), the effect is further explained. As link stiffness increases, the tension in each link relative to the first link tension, drops dramatically.

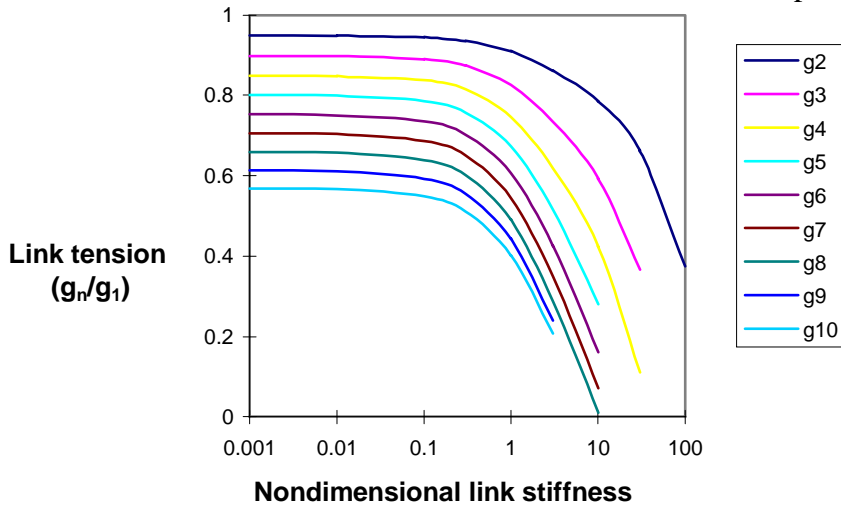


Figure 3-21. Link tension as a function of link stiffness for multiply linked two stereocilia scenario.

Buckling was seen to occur when link stiffness was increased or when the number of links was increased. As links are added under constant link stiffness, or as link stiffness is increased with a constant number of links, the first link to buckle is always the lowest one. As link

stiffness increased, the number of links able to contribute decreased. For stiff links, there is a limited space in which lateral links can contribute stiffness to the bundle. The stiffer the links get, the smaller this space gets. Hence, we see that lateral links must be placed at the top of stereocilia to function mechanically.

Once again we use *bmod* to check these results with tapered anisotropic cilia. As in the two link case, the cilia taper in the last 10% of assembly height to one third the body diameter. The shear modulus was one thousandth of the isotropic value. Diameter to tallest cilia height ratio was 0.02. Link distribution was as above. Results are seen below in figure 3-22. By having tapered anisotropic cilia, deformation profiles flatten enabling links to maintain tension both lower on the cilia, and with a higher link tension. However, tensions still decrease, and indicate for links 10 to 100 times stiffer than the cilia, there is a limited range of link usefulness.

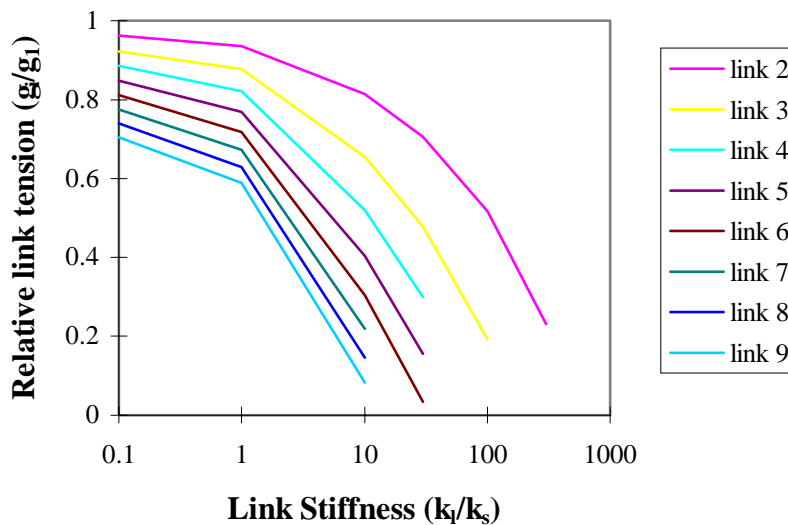


Figure 3-22. Link tension results of two cilia, nine-link model on biologically realistic cilia.

Two non-collinear stereocilia

All models so far have had stereocilia collinear with each other and the applied force. Biologic bundles are arrayed in three dimensions with stereocilia arranged in hexagonal packing. The following scenario (Figure 3-23), will help to gain insight in the stiffness contribution of a stereocilium not attached directly behind the forced stereocilium.

Furthermore, biologically, hair cell bundles respond differently to forces off the E-I axis. This scenario can contribute understanding to the situation where a column is forced, off-axis. Nonlinear responses have been observed to off-axis forces; how much of them is channel opening mechanics and how much is based on the mechanics of the bundle geometry has yet to be determined.

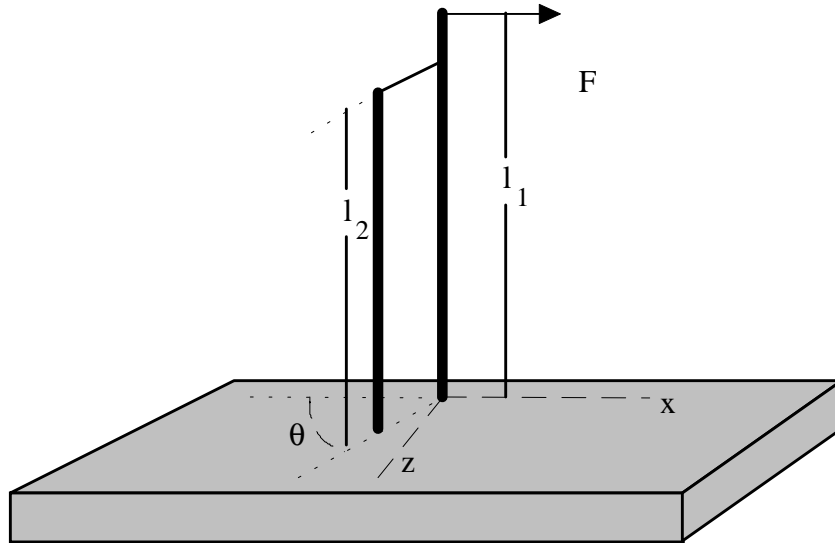


Figure 3-23. Off-axis forcing of two singly linked cilia.

Below is plotted the stiffness of this assembly as a function of tip displacement, for a case with an initial angle of 60 degrees. This implies significant stiffening of bundle-like structures can be realized by the hexagonal packing. As the assembly moves, the second cilia moves in line with the first in a twisting geometry, further stiffening the assembly.

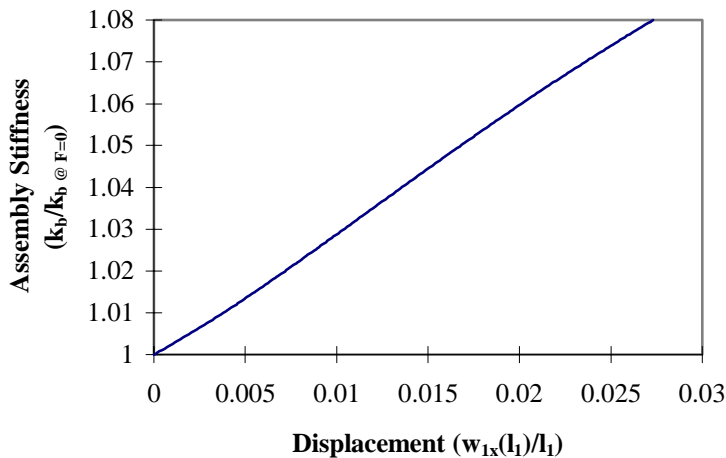


Figure 3-24. Stiffness vs. displacement magnitude for two non-collinear stereocilia. ($k_t/k_s = 0.347$, $l_2/l_1 = 0.9$, $l_0/l_1 = 0.024$, $\theta = 60$ degrees) Relative link stiffness is low because stereocilia are isotropic and untapered making them stiffer plus the link's diameter was reflective of one biologic link, but is 5 times too long ($E = 3 \times 10^6 \text{ N/m}^2$, $d = 5 \text{ nm}$).

Another interpretation of the above solution can be made. Below we see a plot of stiffness verses force angle. This implies the mechanical structure may play some part in the directional sensitivity of hair cell bundles.

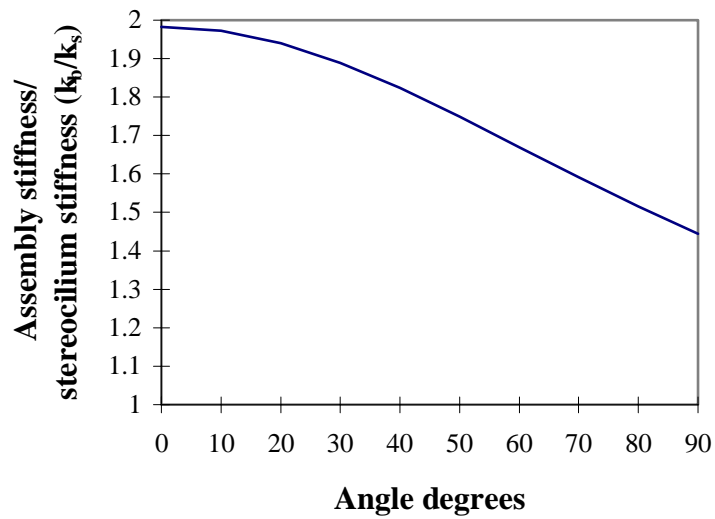


Figure 3-25. Stiffness verses force angle for two non-collinear stereocilia.

Sample Bundle

The same fourteen stereocilia sample bundle that was used to verify the model was used to test several of the conclusions reached earlier. While this bundle does not reflect any actual bundle found in nature, it captures the three-dimensional array aspect of the cilia, as well as the combined side links and tip links that constitute biologic bundles.

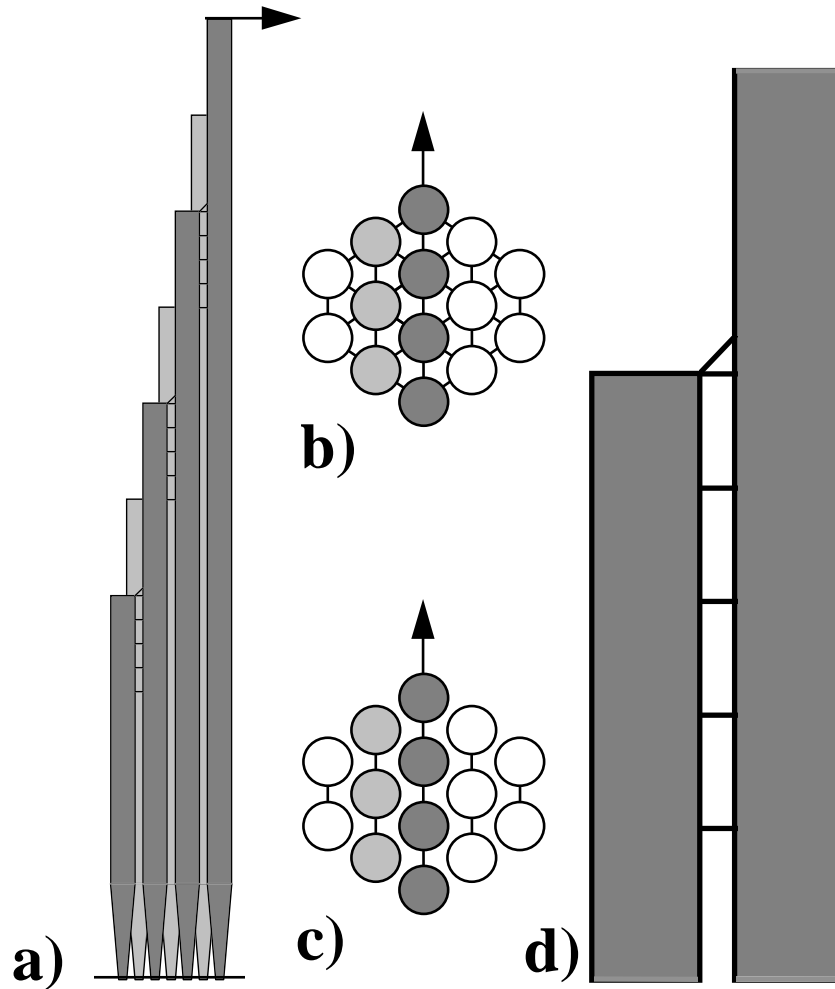


Figure 3-26. Sample bundle used to test several aspects of bundle mechanics. There are 14 stereocilia of linearly decreasing heights. In a) we see the side view of the bundle cilia of two center columns, to show the height distribution and geometry. In b) we see the top view depicting the geometric arrangement of cilia, and distribution of subapical bands. The shaded cilia correspond to the columns shown in a). In c) we see the distribution of tip links. In d) is a detail of the attachment of the lateral links.

Unless otherwise mentioned, the dimensions and properties of the sample bundle are as defined in the table in Appendix B.

The first study done was to vary link stiffness and shear modulus and observe deformed shapes. As with the two cilia model presented earlier, low link stiffness resulted in the bundle splaying apart (figure 3-27a). Link stiffness needs to exceed stereocilia stiffness by several orders of magnitude in order to result in realistic deformations. Another important observation is when shear modulus is too low, a “knee” results in the deformed profile at the first attachment point for the tallest stereocilium (figure 3-27 b). A biologically realistic deformation was obtained as shown in figure 3-27c.

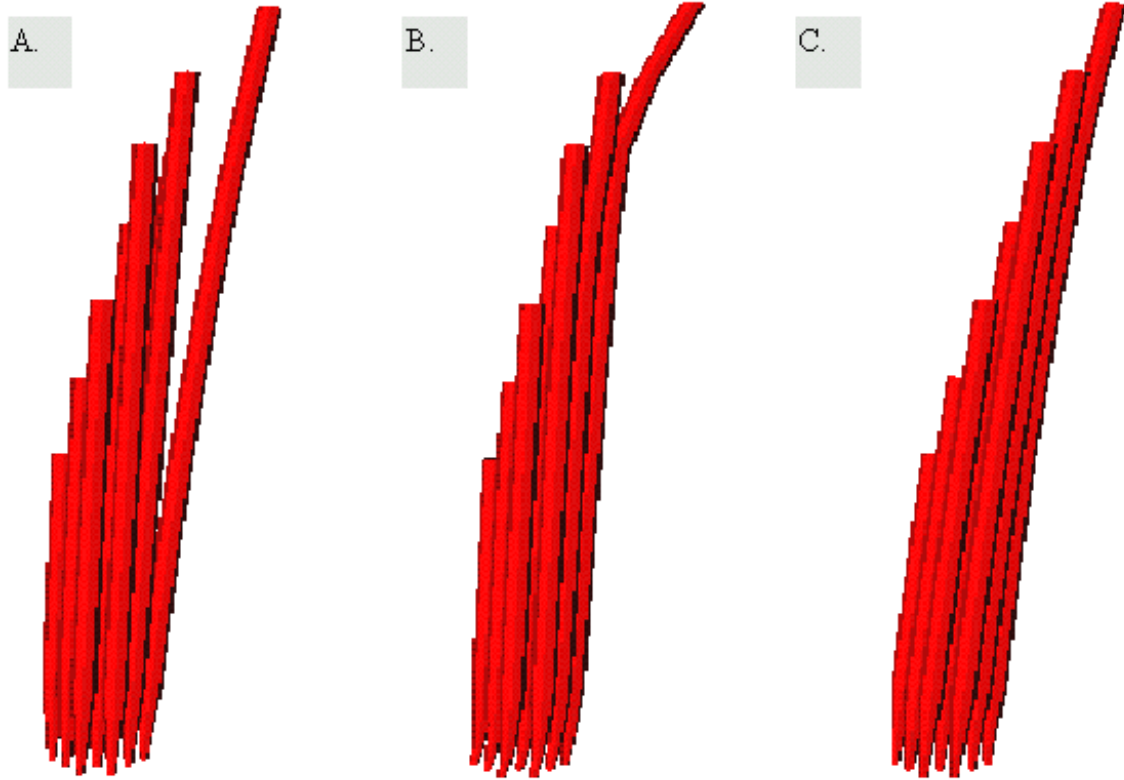


Figure 3-27. Modeled results of the sample bundle. Part A. ($E/G = 10^{-3}$, $k_l/k_s = 10^{-1}$) depicts splay because links are too compliant. Part B. ($E/G = 10^{-5}$, $k_l/k_s = 10^2$) shows how the tallest cilia will “knee” if shear modulus is too low. Part C. shows a biologic deformation profile. ($E/G = 10^{-3}$, $k_l/k_s = 10^2$).

Bundle stiffness for various values of shear modulus and link stiffness are plotted in figure 3-28. The plot of the full bundle shows the same sigmoidal shape as the two stereocilia model (figure 3-6). The top portion of the curve ($k_l/k_s > 10^0$) is more gradual than the two stereocilia case, indicating some splay in successive stereocilium for $k_l/k_s < 10^4$. Tip link stiffness was capped at $10^2 k_s$ to prevent buckling. All bundle stiffnesses presented here, upon dimensionalization, are within the range of biologically reported values of 10^{-2} to 10^{-4} N/m (Szymko, et.al., 1992).

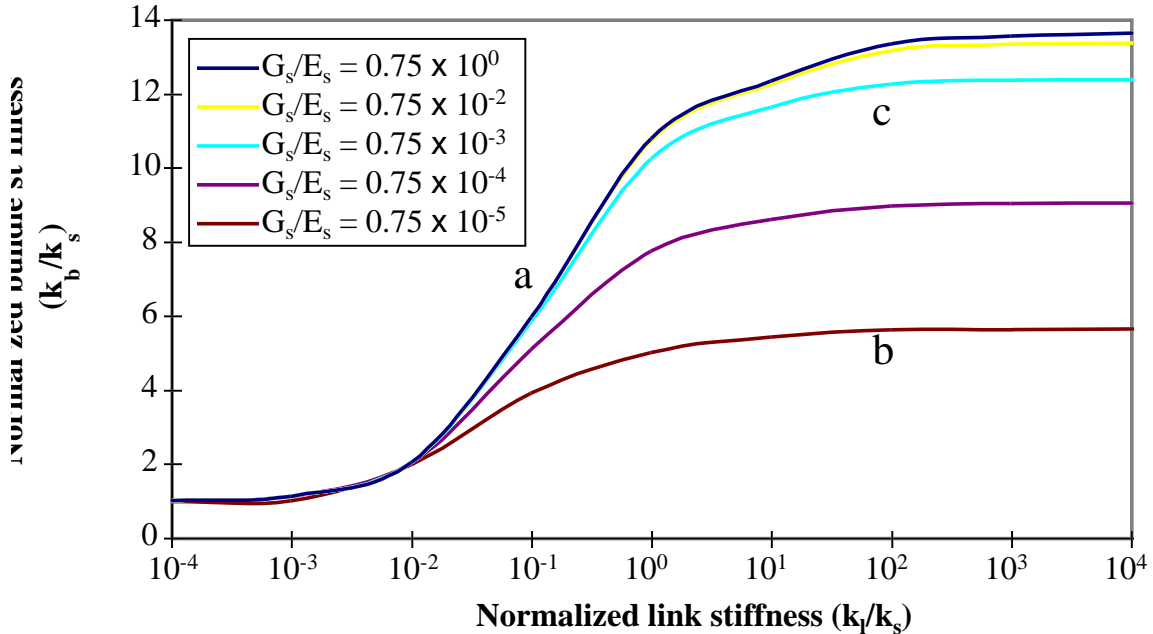


Figure 3-28. Bundle stiffness verses link stiffness and shear modulus. The letters a), b), and c) correspond to the shapes in figure 3-27.

When looking at tip link tensions throughout the bundle, tension decreases as distance from kinocilium grows. Figure 3-29 shows the relative tensions of tip links in between cilia.

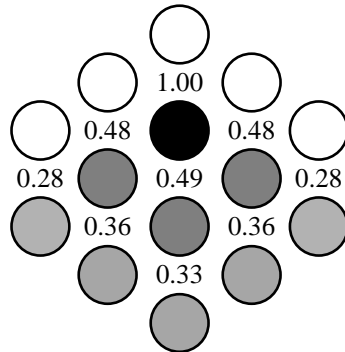


Figure 3-29. Top view of sample bundle ciliary distribution, showing relative tip link tensions for slightly forced bundle. ($F=1pN$)

The combination of geometry and tension decrease may account for the sigmoidal shape of the hair cell response verses displacement curve. For a small force, no tip link tension exceeds the force required to open the gating spring. For a slightly larger force, only the few links near the tallest stereocilia are under enough tension to open the gating spring. As the force grows, not only does the tip link tension increase, but because there are more links (because there are more cilia across) that are receiving this increase in force, the number of links receiving an opening tension increases at a higher rate, resulting in the highest hair cell sensitivity range. As the force further increases, most links in the cilia are open except those few at the end, were the number of ciliary columns tapers back down. Hence the rate decreases once again. Finally, a

force is reached that will open all links, so the cell is saturated, and the response against force is flat.

A test was also performed to test the effect of side link height. The total height at which the side links are found was tested against stiffness. The results are shown below in figure 3-30. Clearly, there is little stiffness change beyond 6 or 7 side links. Furthermore, the stiffness scale of 3-29 shows there is less than a 12 percent change in stiffness between 2 and 10 side links corresponding to side link height of $0.25\ \mu\text{m}$ and $2\ \mu\text{m}$. This further supposes the earlier conclusions of the two stereocilia multi-link models.

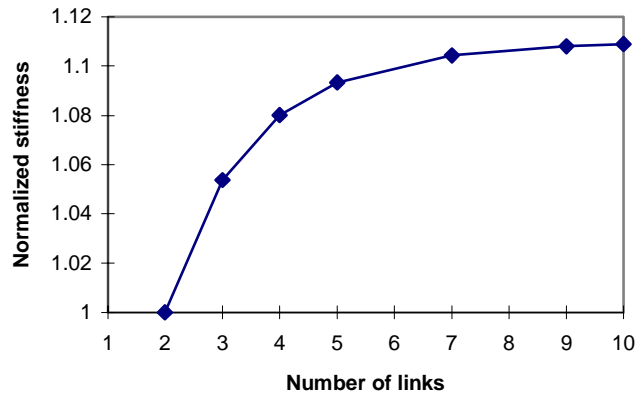


Figure 3-30. Sample bundle stiffness as a function of the total height at which side links are present.

Another test was done by forcing the sample bundles off the excitatory-inhibitory (E-I) axis. Experimental results show a loss of stiffness and hair cell bundle response. Our model shows a loss of 40 percent of the bundle stiffness as the force moves from parallel with the E-I axis to perpendicular to it (figure 3-31). The applied force for these tests was 1 pN.

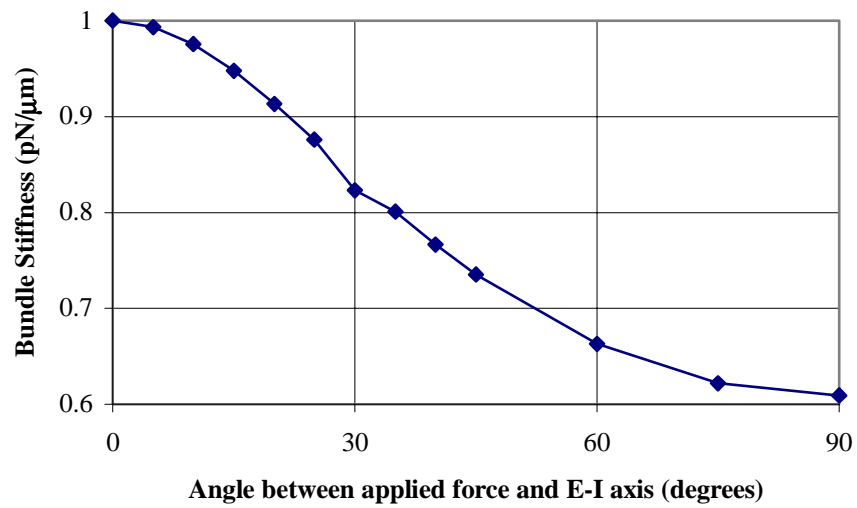


Figure 3-31. Stiffness verses force angle for sample bundle.

Summary

A number of conclusions have been drawn from the preceding models of varying complexity. These are summarized in the table below.

Simplified Model	Discovery
One Stereocilia with no taper, isotropic	Height and diameter dominates stiffness Provides value for nondimensionalization
no taper, anisotropic	Shear deformation reduces stiffness and shallows deformation profile
taper, anisotropic	Taper further reduces stiffness and flattens deformation profile Reduces shear deformation for identical tip deflection magnitude
Two stereocilia with one link	Links must be stiffer than cilia to give biologically observed deformations to pass significant tension through links.
two links	Second lateral link must be near top of cilia to have mechanical relevance Links cannot be too stiff or all lower links lose relevance
many links	Verifies above, only sharpens effect
Column of stereocilia with one link	Stiffness increases with first few stereocilia, then adding cilia has little effect Link tension decreases after n in column
Off-axis forced, two cilia with one link	Stiffness increases with increasing deflection as lateral rows rotate into stiffer configuration. Reduction in stiffness as column is forced off the E-I axis.
Three dimensional bundles	Verifies results of simple models. Lower limit on G identified in order to avoid knee in forced cilia.

There are several values of parameters that we can begin to bracket as a result of these tests. Shear moduli below 10^{-5} of Young's moduli result in too much shearing in the portion of the forced cilium that extends beyond the top of the rest of the bundle. The Young's modulus of strands of actin fibers which make up the stereocilia has been reported as 3×10^9 N/m² [Gittes, 1993]. Therefore, the shear modulus of the stereocilia must exceed approximately 10^4 N/m².

Link stiffnesses must exceed the stereocilium stiffness or the bundle splays. The stiffness of a 10 μ m stereocilium of biologic dimensions was 0.17×10^{-3} N/m, which results in a minimum link stiffness value of the same magnitude. Our model considered the link length to be 0.04 μ m, making the product of the link's Young's modulus and cross sectional area a minimum of roughly 4 N. If side links have an diameter of 5 nm, the modulus of the links must be at least

10^5 . The modulus of the links is suspected to be approximately 3×10^6 N/m² [Howard, et.al., 1988] which is near that of elastin. However, by having multiple links, this requirement could be relaxed.

Much time has been spent studying the effect of having more or less side links present and the location of their distribution. The models have shown there is little mechanical relevance in side links extending below the first micron or so from the top of each cilia. Having them extend lower, does not have an effect. Hence, conclusions about bundle mechanics are very robust to changes in side link configurations. Therefore, despite the dearth of quantitative data reflecting side link structure, the conclusions we draw about bundles are valid. Another interesting comment is that several observations of side links have limited their presence to the top region. This may reflect a certain amount of biological economy in placing bands only where advantageous.